A study concerning the influence of the relative turbulence intensity on local-scour holes

Report W-DWW-93-251

G.J.C.M. Hoffmans
Road and Hydraulic Engineering Division
P.O. Box 5044
2600 GA Delft, Netherlands

february, 1993

A study concerning the influence of the relative turbulence intensity on local-scour holes

Ministry of Transport, Public Works and Watermanagement

Directorate-General of Public Works and Watermanagement

Road and Hydraulic Engineering Division

Voor u ligt een rapport (W-DWW-93-251) dat een modificatie geeft betreffende de turbulentiecoëfficiënt in de Delftse ontgrondingsformule.

In de zestiger jaren is een semi-empirische relatie ontwikkeld om ontgrondingen te voorspellen ten behoeve van de dimensionering van de Deltawerken in Zeeland. In de jaren zeventig en tachtig zijn verschillende bureaustudies uitgevoerd om bovengenoemde turbulentiecoëfficiënt als functie van geometrische parameters zoals lengte van de bodembescherming en drempelhoogte van de constructie etc. te modelleren. Deze relaties hebben een zuiver empirisch karakter, waardoor extrapolatie met grote voorzichtigheid dient te geschieden.

In dit rapport wordt een relatie afgeleid voor de turbulentiecoëfficiënt, welke is gebaseerd op de transportvergelijkingen van de turbulente kinetische energie en de dissipatie. De theorie is geverifieerd door gebruik te maken van meer dan 500 gootexperimenten.

Gijs Hoffmans
7 maart 1993

CONTENTS

List of symbols

b	=	length of the abutment	[L]
B	=	width of the flow	[L]
c_1	=	coefficient	[-]
c_λ	=	relaxation coefficient (= 1.2)	[-]
c_μ	=	coefficient in k-ϵ-model (= 0.09)	[-]
c_0	=	coefficient (= 1.45)	[-]
C	=	Chézy coefficient	[$L^{½}T^{-1}$]
C_k	=	coefficient	[-]
d	=	particle diameter	[L]
D	=	height of the sill	[L]
f_C	=	roughness function	[-]
Fr	=	Froude number $\left(= \overline{U_0}(gh_0)^{-0.5}\right)$	[-]
g	=	acceleration of gravity	[LT^{-2}]
h_0	=	initial flow-depth	[L]
k	=	(kinetic) turbulence energy	[L^2T^{-2}]
k_b	=	(kinetic) turbulence energy close to the bed (non-uniform flow)	[L^2T^{-2}]
k_m	=	(kinetic) turbulence energy in the mixing layer	[L^2T^{-2}]
k_s	=	equivalent (or effective) roughness of Nikuradse	[L]
k_0	=	(kinetic) turbulence energy close to the bed (uniform flow)	[L^2T^{-2}]
k_η	=	(kinetic) turbulence energy in relaxation zone	[L^2T^{-2}]
K	=	coefficient	
K_1	=	coefficient	[-]
L	=	length of the bed protection	[L]
n	=	number	[-]
Q	=	discharge	[L^3T^{-1}]
r_0	=	relative turbulence intensity	[-]
R	=	hydraulic radius	[L]
Re	=	Reynolds number $\left(= \overline{U_0}h_0/\nu\right)$	[-]
t	=	time	[T]
t_1	=	characteristic time at which $y_m = h_0$	[T]
T_α	=	transport parameter $\left(= (\alpha\overline{U_0} - \overline{U_c})/\overline{U_0}\right)$	[-]
u'	=	longitudinal turbulent velocity component	[LT^{-1}]
u_*	=	bed shear-velocity	[LT^{-1}]
u_{*c}	=	critical bed shear-velocity	[LT^{-1}]
$\overline{U_c}$	=	depth-averaged critical flow-velocity according to Shields	[LT^{-1}]
$\overline{U_0}$	=	mean flow-velocity $\overline{U_0} = Q/(B\,h_0)$	[LT^{-1}]
v'	=	transverse turbulent velocity component	[LT^{-1}]
w'	=	vertical turbulent velocity component	[LT^{-1}]
x	=	longitudinal coordinate	[L]
x_R	=	x-coordinate where the flow reattaches the bed	[L]
y_m	=	maximum scour-depth	[L]
α	=	turbulence coefficient	[-]
α_k	=	coefficient (= -1.08)	[-]

β_l	=	coefficient	[-]
β_k	=	coefficient (= 0.5)	[-]
β_m	=	angle of the mixing layer (= 0.09)	[-]
γ	=	coefficient (= 0.3 to 0.4)	[-]
ϵ	=	error rate	[-]
Δ	=	relative density $(= (\rho_s - \rho)/\rho)$	[-]
κ	=	constant of von Kármán (= 0.4)	[-]
λ	=	relaxation length $(\approx \frac{1}{2}\, c_\lambda h_0/\beta_m)$	[L]
ρ_s	=	material density	$[ML^{-3}]$
ρ	=	fluid density	$[ML^{-3}]$
σ	=	standard deviation	[-]
ν	=	kinematic viscosity	$[L^2T^{-1}]$
ω_b	=	coefficient (= 0.3)	[-]

Subscripts

c	=	calculated
i	=	index
m	=	measured
R	=	rough
S	=	smooth
0	=	initial

1 Introduction

Scour is the lowering of the sea or river-bed as a result of non-equilibrium sediment transport conditions and can be divided into several categories (Breusers and Raudkivi, 1991). Local scour, which may occur at the base of a structure because of the affected flow pattern, can severely endanger the stability of this structure. Many varieties of local-scour systems downstream from hydraulic structures exist, each with its own particular geometry and hence local scour mechanism. Local scour is superimposed on general and constriction scour.

The prediction of local-scour holes that develop downstream from hydraulic structures plays an important role in their design. Excessive local scour can progressively undermine the foundation of a structure. Because complete protection against scour is too expensive generally, the maximum scour-depth and the upstream slope of the scour hole have to be predicted to minimize the risk of failure.

In 1961 a systematical research with respect to scour holes started at Delft Hydraulics within the scope of the Dutch Delta works. After the catastrophic flood disaster in 1953 the Delta plan was made to protect the Rhine-Meuse-Scheldt delta for future disasters. Dams with large scale sluices were planned in some estuaries. The severe scour expected necessitated a better understanding of the scour process.

To find detailed information about the physical processes playing a role in scour many experiments were carried out, in which various parameters of the flow and the scoured material were varied. From the results of experiments in flumes with all difficulties of scale effects and limitations in instrumentation some empirical relations were obtained, which describe the erosion process as function of time and place (Prins, 1963 and Breusers, 1966, 1967).

In these empirical relations a not well defined turbulence coefficient was introduced. Up to now this coefficient was related to the geometry upstream of the scour hole, which relation was based on trial and error. Based on theoretical grounds an analytical relation for the depth-averaged turbulence intensity is derived. This relation, which implies a modification of the turbulence coefficient in the Breusers scour formula, is verified using approximately 300 experiments.

The modified scour formula yields results that compare reasonably well to measured and computed developments of a scour hole in case of a uniform flow upstream of the scour hole corresponding with a large protected bed area. The computations were based on the two-dimensional Navier-Stokes and convection-diffusion equations (Hoffmans, 1992). The present paper aims at extension of the domain of application of the scour formula to non-uniform flow conditions upstream.

2 Semi-empirical scour relations

Generally the scour process is determined by flow and sediment characteristics. The sediment transport is mainly dependent on the bed shear-stress and the turbulence condition near the bed on the one hand and the density of the bed material, the

sediment-size distribution and the porosity of the (non-cohesive) material on the other hand. Based on many clear-water scour observations Breusers (1966, 1967) reported that the scour process could be written as:

$$\frac{y_m}{h_0} = \left[\frac{t}{t_1}\right]^{\gamma} \quad \text{where} \quad t_1 = \frac{K\,\Delta^{\beta_2}\,h_0^{\beta_3}}{\left(\alpha\overline{U_0} - \overline{U_c}\right)^{\beta_1}} \tag{1}$$

or using the invariables g (acceleration of gravity) and ν (kinematic viscosity), t_1 (i.e., characteristic time at which $y_m = h_0$) can also be given by:

$$t_1 = \frac{h_0}{\overline{U_0}}\,\frac{K_1\,\Delta^{\beta_2}}{T_\alpha^{\beta_1}\,Fr^{\beta_4}\,Re^{\beta_5}} \tag{2}$$

In the equations above y_m is the maximum scour-depth, h_0 is the initial flow-depth, t is the time, $\overline{U_0} = Q/(Bh_0)$ is the mean flow-velocity, Q is the discharge, B is the width of the flow, $\overline{U_c}$ is the depth-averaged critical flow-velocity (Shields), $\Delta = (\rho_s - \rho)/\rho$ is the relative density, ρ_s is the material density, ρ is the fluid density, $T_\alpha = (\alpha\overline{U_0} - \overline{U_c})/\overline{U_0}$ is a transport parameter, $Fr = \overline{U_0}(gh_0)^{-0.5}$ is the Froude number, $Re = \overline{U_0}h_0/\nu$ is the Reynolds number and K, K_1 and α are coefficients (table 1). Originally the characteristic time t_1 was expressed in hours (Breusers, 1966), so that the dimension of K measured [hours $m^{\beta_1-\beta_3}\,s^{-\beta_1}$], $\left(3600K = K_1 g^{\frac{1}{2}\beta_4}\nu^{\beta_5}\right)$

	K	$K_1/10^6$	β_1	β_2	β_3	β_4	β_5	α
Hinze (1961)	90	0.94	4.0	1.62	2.05	2.7	0.3	$1+3r_0$
Breusers (1966, 1967)	90	0.94	4.0	1.62	2.05	2.7	0.3	$1+3r_0$
Dietz (1969)	48	9.96	4.0	1.5	1.75	2.5	0.5	$1+3r_0$
van der Meulen and Vinjé (1975)	250	12.9	4.3	1.7	2.0	2.87	0.43	
Zanke (1978)			4.0	1.33	2.0	2.67	0.33	
de Graauw and Pilarczyk (1981)	330	17.1	4.3	1.7	2.0	2.87	0.43	
Jorissen and Vrijling (1989)	330	17.1	4.3	1.7	2.0	2.87	0.43	$1.5+5r_0$

Table 1 Empirical coefficients in scour formula (equations 1 and 2)

The sediment transport (bed load and suspended load) is largely determined by the bed turbulence during the fluid inrush phase (sweeps) and the turbulent outrush phase (ejections). During the turbulent outrush phase the bed layer is disrupted locally by bursts of fluid, so that then the sediment particles are in suspension. In the transport parameter T_α, which can be interpreted as a measure for the erosion capacity in the scour hole, the turbulence is represented by the turbulence coefficient α. According

to Hinze (1961) the turbulence coefficient α is related to r_0 (i.e., relative turbulence intensity) at the transition of the fixed to the erodible bed. Hence the local bed turbulence in the scour hole is not included in α. Though this is somewhat controversial, the used approach is followed because of its simplicity. In section 4.4 a comprehensive analysis is given regarding turbulence parameters in non-uniform flow. Zanke (1978) has given a clear definition of the different scour phases. He assumed that the scour process can be divided in four phases. In the first phase a scour hole arises, in which the maximum scour-depth increases progressively compared to the corresponding longitudinal distance x_m, i.e., the distance from the end of the bed protection to the point where the scour hole is at maximum. In the second phase the forms of the scour hole are similar. Then the ratio y_m/x_m is more or less constant. In the third phase the development of the scour depth increases depressively and in the last phase an equilibrium is achieved, figure 1.

For three-dimensional scour the coefficient γ is dependent on the geometry (van der Meulen and Vinjé, 1975).

The definition of the exponent γ in equation (1) is not obtained unambiguously. For two-dimensional flow the coefficient γ measures about 0.38, which is based on an extensive analysis of the bed levels measured at which the maximum scour-depth is about $0.5h_0$. A smaller value of γ (=0.32) is more appropriate for experiments, where the maximum scour-depth is approximately equal to the initial flow-depth. According to Dietz (1969) the coefficient γ lies in the range of 0.34 to 0.40, which can be considered as a confirmation of the Breusers' results. When the time boundaries of the second phase of the scour process are more specified, the value of γ might be more unambiguously. To include the time evolution of local scour γ was assumed to be $\gamma = 10^{-0.1y_m/h_0 - 0.3}$ (Driegen et al., 1987).

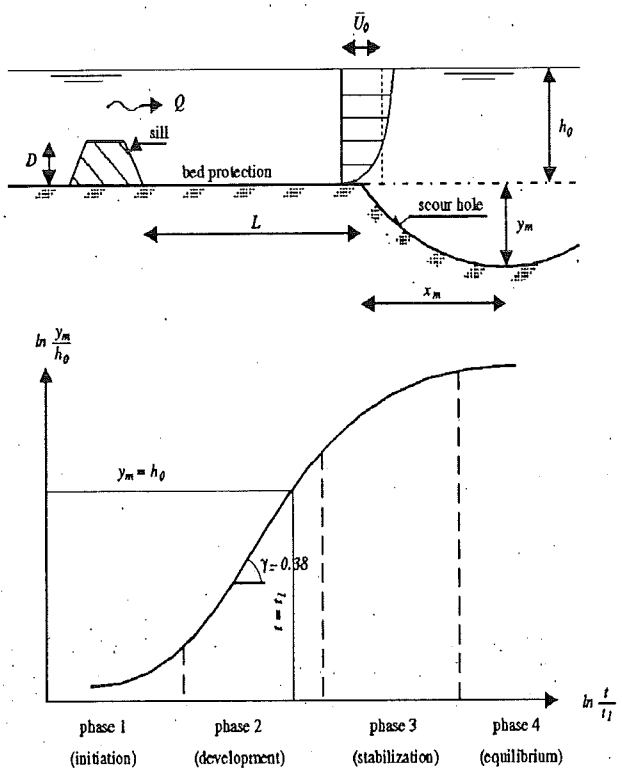

Figure 1 Development of the scour process

After a further extensive evaluation of the enormous amount of data of both two and three-dimensional scour experiments the coefficients in the scour relations were readjusted (van der Meulen and Vinjé, 1975; de Graauw and Pilarczyk, 1981 and Jorissen and Vrijling, 1989). Besides these Dutch research activities many other investigators (Dietz, 1969 and Zanke, 1978) contributed to the solving of the problem of scour with empirical relations. The research activities of Dietz and Zanke (Hoffmans, 1992) confirmed the considerations of Breusers. Although the formulae are identical, Dietz proposed different values for the empirical coefficients (table 1). The differences

between the coefficients obtained by calibrating the measurements are small and may be due to the different method calculation, where the number of experiments and the reach of the hydraulic and material parameters are not insignificant considering the 'improved' constants.

3 Initiation of movement

In 1936, Shields published his criterion for beginning of movement of uniform granular material on a flat bed. The experimental data used by Shields was mostly obtained by extrapolating curves of sediment transport versus applied shear stress to the zero transport condition. Originally the data points were plotted by Shields and the curve (averaged critical value) was drawn by Rouse constituting the 'Shields diagram' as usually quoted (Neill, 1968). Actually Shields drew not a single curve, but a broad belt for reasons of the non-uniform distribution of the mixtures and the effects of grain and imbrication (i.e., the preferred orientation of natural sands and gravel particles under certain conditions of transport.
In the sixties Delft Hydraulics studied the initiation of movement of bed material in detail and distinguished seven qualitative criteria. These introduced criteria all lie in the broad belt as given by Shields originally confirming the earlier research activities of Shields.
To determine the critical bed shear-velocity $u_{*,c}$ a criterium was selected, which was characteristic for a flow in which the bed particles move permanent at every location. This criterium almost agreed with the averaged critical value drawn by Rouse.
The critical bed shear-velocity can be obtained graphically directly from the Shields diagram. However, to avoid more than one possible interpretation $u_{*,c}$ can also be determined using analytical expressions (e.g., van Rijn, 1984), which fit the Shields diagram. With the aid of Chézy's formula and applying the Chézy coefficient, as proposed by Thijsse (1949), the depth-averaged critical flow-velocity reads:

$$\overline{U_c} = u_{*,c}\frac{C}{\sqrt{g}} \tag{3}$$

$$C = \frac{\sqrt{g}}{\kappa}\ln\left[\frac{12R}{k_s + \dfrac{3.3\nu}{u_{*,c}}}\right] \tag{4}$$

in which C is the Chézy coefficient, κ is the constant of von Kármán, R is the hydraulic radius and k_s is the equivalent (or effective) roughness of Nikuradse.
Usually the equivalent roughness of a plane bed is related to the largest particles of the bed d_{65}, d_{84}, d_{90}. The influence of the gradation, the shape of the particles and the flow conditions are generally disregarded. In the systematical research on scouring the equivalent roughness was taken equal to the mean particle diameter. However, in the literature several values for k_s can be found, table 2. According to van Rijn (1982) the

equivalent roughness of a plane movable bed varies from about 1 to 10 times d_{90} of the bed material. These values, which are rather large, show that a completely plane bed does not exist for conditions with active sediment transport. Probably, the relatively large scatter of the equivalent roughness is caused by the initial unevenness (initial bed forms). Here the equivalent roughness is supposed to be twice as large as the mean particle diameter, which almost agrees with the assumption made by Engelund-Hansen.

	k_s
Ackers-White	$1.25d_{35}$
Einstein	d_{65}
Engelund-Hansen	$2d_{65}$
Hey	$3.5d_{84}$
Kamphuis	$2.5d_{90}$
Mahmood	$5.1d_{84}$
van Rijn	$3d_{90}$

Table 2 Equivalent roughness (van Rijn, 1982)

4. Turbulence parameters

4.1 *General*

Usually a sill has the function of a foundation for a closure dam in an alluvial river or estuary. In a river the flow over a sill is mostly unidirectional. Sills with a broad or a sharp crest and a sill with and without a bed protection can be distinguished. Normally the flow above a sill is subcritical, but depending on the waterlevel downstream from the sill the flow can become supercritical. In this study only subcritical flow is considered.

4.2 *Nature of the flow*

In analogy of the distribution of characteristic flow patterns in scour holes (Hoffmans, 1992) the following flow zones can be distinguished downstream from a sill: a mixing layer, a recirculation zone, a relaxation zone and a new wall-boundary layer, figure 2. In the deceleration zone, the separated shear-layer appears to be much like an ordinary plane mixing layer. A recirculating flow develops behind the sill. The underside of the shear layer curves sharply downwards to the reattachment point. Both in the mixing layer and in the recirculation zone the flow is very unsteady and highly turbulent. Downstream from the point of

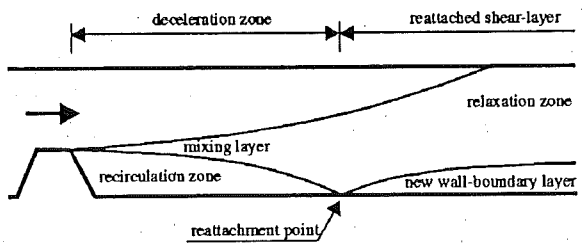

Figure 2 Flow regions

reattachment, the turbulence energy and the dissipation rate of the turbulence energy decay rapidly. Simultaneously, a new wall-boundary layer develops and spreads into the relaxation zone (the outer part of the reattached shear-layer). Measurements of Troutt et al. (1984) have shown that behind a backward-facing step the flow in the relaxation zone still has most of the characteristics of a free shear layer flow as much as 50 step heights downstream from reattachment. This observation demonstrates the persistence of the large-scale eddies, which are developed in the mixing layer.

4.3 *Turbulence energy and turbulence intensity*

Based on theoretical grounds a relation is derived for the turbulence coefficient α in the transport parameter in equation 1 (section 4.4). In this relation α is related to r_0 at the transition of the fixed to the erodible bed. The parameter r_0 is the depth-averaged relative turbulence intensity of the longitudinal turbulence velocity component. The longitudinal component is only considered because this was the only component measured in general.

Before examining the turbulence energy downstream from a sill in more detail some definitions are given. The (kinetic) turbulence energy k and r_0 respectively are defined by (Hinze, 1975):

$$k = \tfrac{1}{2}\left(\overline{u'u'} + \overline{v'v'} + \overline{w'w'}\right) \tag{5}$$

$$r_0 = \frac{1}{\overline{U_0} h_0} \int_0^{h_0} \sqrt{\overline{u'u'}(z)}\, dz \tag{6}$$

in which the terms u' , v' and w' represent the fluctuating flow-velocities in the longitudinal, transverse and vertical direction respectively.

Combining equations (5) and (6) and using measurements of Nezu (1977) the turbulence energy (averaged over the depth) is for uniform-flow (Appendix A):

$$\frac{1}{h_0} \int_0^{h_0} k(z) dz \simeq \left(r_0 \overline{U_0}\right)^2 \tag{7}$$

For non-uniform flow, measurements of van Mierlo & de Ruiter (1988) have shown that the turbulence energy k_m in the centre of the mixing layer grows rapidly to a maximum. Downstream from the point of reattachment the turbulence energy in the relaxation zone decreases gradually again and becomes small compared to the turbulence energy k_b generated by the bed in the developing new wall-boundary layer. The turbulence energy generated in the mixing layer vanishes for relatively large values of x , i.e., where the new wall-boundary layer is well developed. Then the turbulence energy tends to an equilibrium value k_0 , which largely consists of turbulence generated at the bed.

Earlier studies of Hoffmans (1992) have shown that in a scour hole k_b can be represented by a combination of the turbulence energy generated at the bed and a certain

part of the turbulence energy from the mixing layer, figure 3.

$$k_b(x) = \omega_b k_\eta(x) + k_0(x) \quad \text{where} \quad k_0(x) = \frac{u_*^2(x)}{\sqrt{c_\mu}} \tag{8}$$

where ω_b ($\simeq 0.3$) is a turbulence coefficient, u_* is the bed shear-velocity and c_μ (=0.09) is a coefficient used in k-ϵ-models (Rodi, 1980).

To analyze the decay of the turbulence energy in the relaxation zone an analogy with the decay of k and the dissipation in grid turbulence can be used (Launder and Spalding, 1972). When the zone downstream from the point of reattachment is considered and the production and diffusion terms in the transport equations of the turbulence energy and the dissipation are neglected, k_η can be given by (Hoffmans, 1992):

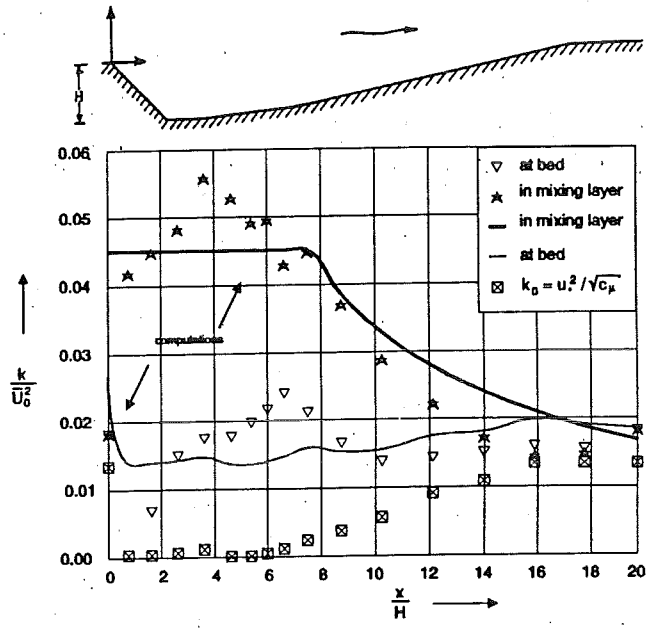

Figure 3 Calculated and measured k as function of x above an artificial dune (van Mierlo & de Ruiter, 1988)

$$k_\eta(x) = k_m \left(\frac{x - x_R}{\lambda} + 1 \right)^{\alpha_k} \tag{9}$$

in which x is the longitudinal coordinate, x_R ($\simeq 6D$) is the x-coordinate where the flow reattaches the bed, D is the height of the sill, λ ($\simeq \frac{1}{2} c_\lambda h_0/\beta_m$) is a relaxation length, β_m (=0.09) is the angle of the mixing layer, c_λ (=1.2) is a relaxation coefficient and α_k (=-1.08) is a coefficient, which is directly related to the turbulence coefficients used in k-ϵ-models.

The hypothesis of self-preservation (Townsend, 1976) requires a constant turbulence energy in the mixing layer up to the point where the boundaries have reached the surface and the bed. An appropriate value is (Hoffmans, 1992):

$$k_m = C_k \overline{U}^2 \tag{10}$$

in which C_k (=0.045) is a coefficient and $\overline{U}$ is the depth-averaged flow velocity above the sill.

In analogy of equation (8) the turbulence energy averaged over the depth, from which r_0

can be determined downstream from a sill, can be given by:

$$\frac{1}{h_0}\int_0^{h_0} k(x,z)dz = \beta_k k_\eta(x) + c_0 u_*^2(x) \qquad (11)$$

in which β_k (=0.5) is a coefficient (Appendix B).
Actually the bed shear-velocity varies in the streamwise direction. In the recirculation zone the bed shear-velocity is relatively small and even zero in the reattachment point. Downstream from the point of reattachment the bed shear-velocity tends rapidly to the equilibrium value corresponding to uniform-flow conditions for which applies $c_0 = 1.45$. The length of the bed protection L will for safety reason always extend beyond the point of reattachment. Combining equations (7) to (11) in the zone downstream from the point of reattachment only shows r_0 can be represented by:

$$r_0 = \sqrt{\beta_k C_k \left(1 - \frac{D}{h_0}\right)^{-2} \left(\frac{L-6D}{\lambda} + 1\right)^{\kappa} + c_0 \frac{g}{C^2}} \qquad (12)$$

in which C is the Chézy coefficient related to the bed protection upstream from the scour hole.
More than 250 experiments (Delft Hydraulics, 1972 and Buchko, 1986) were used to verify the model equation for the turbulence intensity. In these laboratory experiments the hydraulic conditions ($\overline{U_0}$, h_0, k_s) as well as the geometrical parameters (L, D, B) were varied (appendix D). Moreover tests were executed with an abutment in permanent flow introducing three-dimensional scour. In these tests the length of the abutment measured $b = 0.1B$, figure 4.
Figures 5 to 8 presents the results of the measured and calculated values of r_0, where the influence of both the height of the sill and the length of the bed protection can be observed.
The standard deviation of r_0 for three-dimensional experiments (figures 6 and 8) is somewhat larger than for two-dimensional ones (figures 5 and 7). This can partly be ascribed to periodical vortices, which can occur at the boundaries of the mixing layer in the transverse direction known as a Kármán Vortex-Street (Vinjé, 1969) and partly to the measuring procedure.

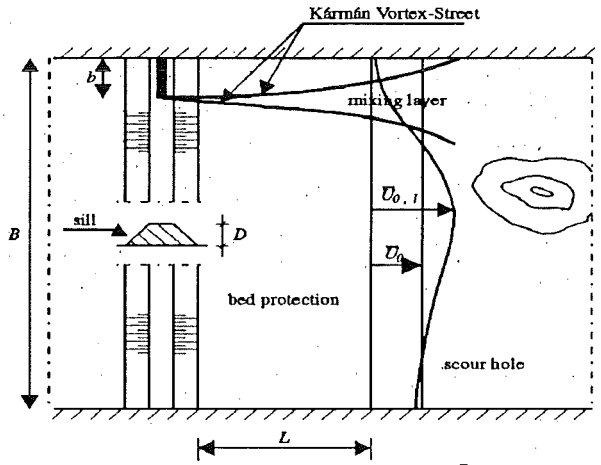

Figure 4 Definition sketch of $\bar{U}_{0,t}$

In the two-dimensional experiments the velocities in the main direction of the flow were

measured with a propellor-type current meter (Schuyf, 1966) and were taken at about 10 points along the vertical axis in the centre of the flume. In the case of three-dimensional scour the longitudinal flow-velocities were also measured at several locations along the transverse axis. However, the data given in figures 6 and 8 are not averaged values over the width of the flume, but concerns measurements carried out in the axis, where the depth-averaged flow velocity is at maximum.

The measurements of the longitudinal flow-velocity near the bed, where large gradients occur, were inaccurate. Due to the relatively large dimensions of the measuring instrument the flow pattern was disrupted introducing severe errors. Also the number of measuring points in the vertical was not enough especially in the mixing layer to calculate r_0 from the measurements accurately (figure 7).

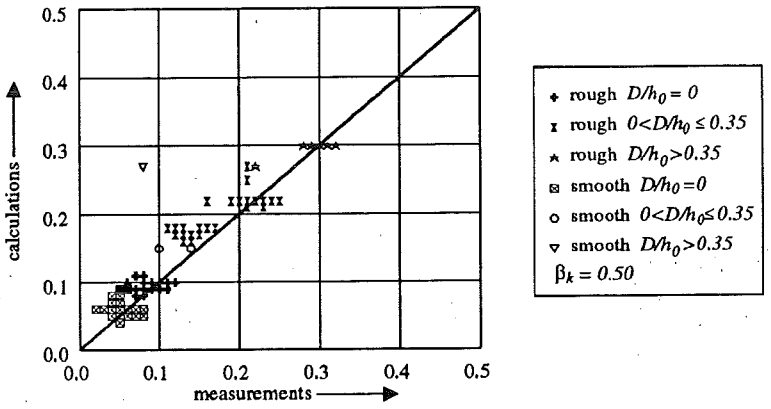

Figure 5 Relative turbulence intensity (2-D experiments)

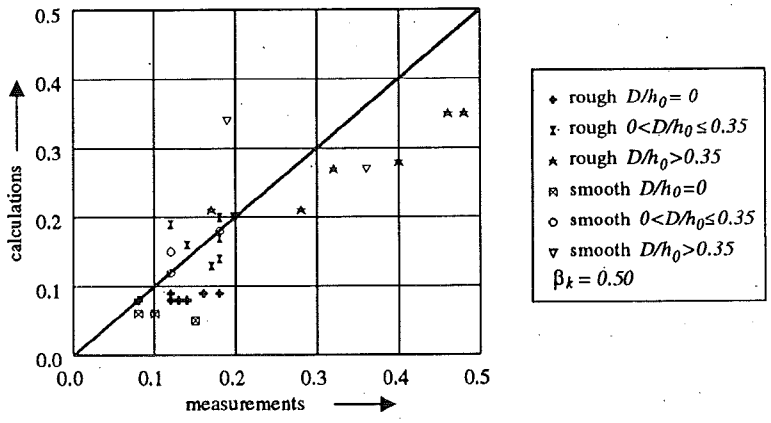

Figure 6 Relative turbulence intensity (3-D experiments)

4.4 *Turbulence coefficient in the scour formula*

The value of α in the scour formula can be obtained using the relation between α and r_0 from Jorissen and Vrijling (1989):

$$\alpha = 1.5 + 5r_0 \qquad (13)$$

This value is based on the use of a local depth-averaged velocity $\overline{U_{0,l}}$ in the scour formula. If a three-dimensional flow is considered and the mean flow-velocity $\overline{U_0}$ (figure 4) is used in the scour formula, the value of α has to be multiplied by $\overline{U_{0,l}}/\overline{U_0}$.

A re-examination of more than 250 experiments (Delft Hydraulics, 1972 and Buchko, 1986) shows that reasonable results are then achieved for both two and three-

dimensional experiments (table B1, appendix B).

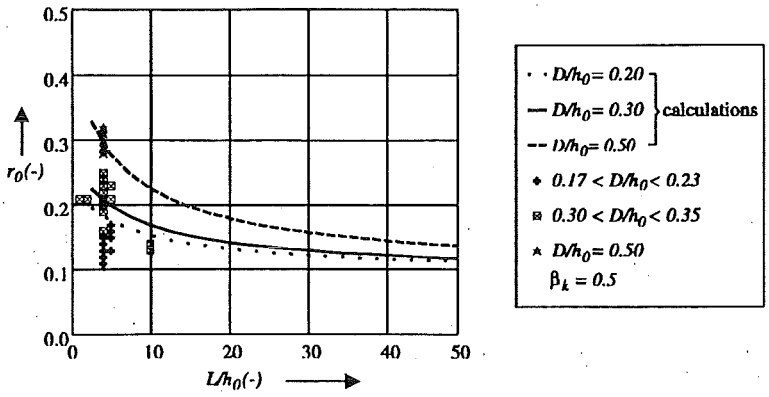

Figure 7 Relative turbulence intensity as function of L/h_0 (2-D experiments; rough)

Already Hinze (1961) remarked that not only the influence of the turbulence intensity but also the influence of the flow-velocity profile near the bed is significant for the development of the scour process. To include the influence of a smooth bed a simple expression is introduced, which is verified applying about 550 experiments (Delft Hydraulics, 1972; Dietz, 1969; Buchko, 1986 and Hoffmans, 1990):

$$\alpha = 1.5 + 4.4 r_0 f_c \qquad (14)$$

in which $f_c = C/C_0$ represents a roughness function and $C_0 = 40\,m^{1/2}/s$. For hydraulically-rough conditions, i.e., for $C \leq 40\,m^{1/2}/s$ regarding the fixed bed before the scour hole, $f_c = 1$.

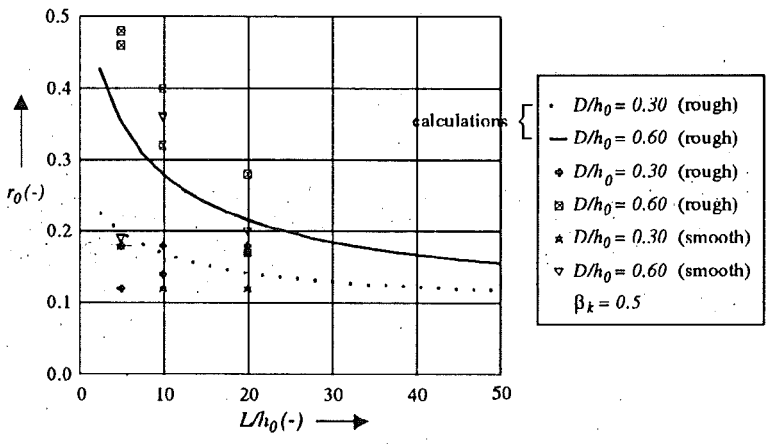

Figure 8 Relative turbulence intensity as function of L/h_0 (3-D experiments)

Though the influence of three-dimensional effects are not included in the model equation for r_0 (equation 12) satisfactory results are obtained, especially for two-dimensional scour (appendix B).

5 Conclusions

A model equation is given for the turbulence coefficient (equation 12) in the Breusers scour formula, which is based on theoretical grounds and fitted to results of velocity measurements. This study shows a way to calculate the relative turbulence intensity at the transition of the fixed bed to the erodible bed, which can be used to predict two-dimensional scour downstream from a sill.

The particular case of scour of three-dimensional flow considered here is flow around an abutment with consequent scour development downstream. Although some char-

acteristics of three-dimensional flow and additional phenomena such as vortices with a vertical axis in particular have not been taken into account in the model equation for the turbulence intensity, promising results regarding three-dimensional scour are obtained. For example, in the centre of the flow where the scour depth is about at maximum, the influence of the Kármán Vortex-Street can be neglected. However, prudence has to be called for complex hydraulic structures. Then it is recommended to carry out experiments using a scale model to find detailed information about the development of a scour hole.

Appendix A **Relation between the depth-averaged turbulence energy and the relative turbulence intensity**

For uniform flow the relative turbulence intensity of the transverse and vertical component can be written as (Nezu, 1977):

$$\sqrt{\overline{v'v'(z)}} = \gamma_v \sqrt{\overline{u'u'(z)}} \tag{A1}$$

$$\sqrt{\overline{w'w'(z)}} = \gamma_w \sqrt{\overline{u'u'(z)}} \tag{A2}$$

in which γ_v (= 0.71) and γ_w (= 0.55) are coefficients.
Combining equations (A1) and (A2) and the definition of the turbulence energy (equation 5), the turbulence energy can be given by:

$$k(z) = c_1 \overline{u'u'(z)} \tag{A3}$$

in which $c_1 \left(= \frac{1}{2}(1 + \gamma_v^2 + \gamma_w^2) \simeq 0.90\right)$ is a coefficient.
The variance of the longitudinal instantaneous flow-velocity reads (Nezu, 1977):

$$\overline{u'u'(z)} = \gamma_u u_*^2 \exp\left[-\frac{2z}{h_0}\right] \tag{A4}$$

in which γ_u (= 1.92) is a coefficient.
Hence the depth-averaged turbulence energy can be given by:

$$\frac{1}{h_0}\int_0^{h_0} k(z)dz = c_2 u_*^2 \tag{A5}$$

in which $c_2 = \frac{1}{2}(1 - e^{-2})c_1\gamma_u^2 \simeq 1.44$.
Applying equation (A4) and the definition of the relative turbulence intensity (equation 6), r_0 can be represented by:

$$r_0 = \frac{c_3 u_*}{\overline{U_0}} \tag{A6}$$

in which $c_3 = (1 - e^{-1})\gamma_u \simeq 1.21$.
Consequently the relation between the depth-averaged turbulence energy and r_0 is:

$$\frac{1}{h_0}\int_0^{h_0} k(z)dz = c_4\left(r_0\,\overline{U_0}\right)^2 \qquad \text{(A7)}$$

in which $c_4 = c_2/c_3^2 \simeq 1.0$.

Appendix B **Optimization of the relative turbulence intensity**

Three methods are used to optimize β_k in equation 12, which are (table B1):

Least Absolute Value Method (LAVM):	$\epsilon_{LAVM}(\beta_k) = \sum_{i=1}^{n} \frac{\lvert r_{0_{e,i}}(\beta_k) - r_{0_{m,i}} \rvert}{r_{0_{m,i}}}$
Least Square Method (LSM):	$\epsilon_{LSM}(\beta_k) = \sum_{i=1}^{n} \left[\frac{r_{0_{e,i}}(\beta_k) - r_{0_{m,i}}}{r_{0_{m,i}}}\right]^2$
Least Standard Deviation Method (LSDM):	$\epsilon_{LSDM}(\beta_k) = \sqrt{\sum_{i=1}^{n} \frac{\left(r_{0_{e,i}}(\beta_k) - r_{0_{m,i}}\right)^2}{n-1}}$

Table B1 Optimize methods

In table B1 $r_{0_{e,i}}$ and $r_{0_{m,i}}$ are the calculated and the 'measured' r_0 respectively. Actually the 'measured' r_0 is not a measurement but calculated using measurements, since the turbulence intensity is here defined as the integration of the measured local turbulence intensities (equation 6). The error function $\epsilon(\beta_k)$ as discussed above is

	β_k	$\sigma(\beta_k)$
LAVM	0.357	0.043
LSM	0.386	0.042
primary estimation	0.500	0.040
LSDM	0.596	0.042

Table B2 Results of the optimize methods regarding β_k

minimized applying n (=285) flume experiments (Delft Hydraulics, 1972 and Buchko, 1986) yielding the following results for β_k, table B2.
From this analysis it can be deduced that r_0 is slightly dependent on β_k. The methods LAVM and LSM reflect the measurements in a better way for relatively small values of r_0 (appendix C). Conversely the method LSDM gives better results for relatively large values of r_0.
Besides this optimization of β_k the standard deviation $\sigma(\beta_k)$ is determined. Overall, the smallest error is obtained for $\beta_k = 0.5$ (table B2).

Appendix C **Optimization of the turbulence coefficient**

The number of laboratory experiments used to find the best compromise among the 'measured' and calculated α in equation (14) using the 'measured' values of r_0, amounts to 285 (Delft Hydraulics, 1972), table C1. Several model relations for α are introduced, which are:

$$\alpha = (1.079 + 5.118 r_0) f_c \qquad \text{(C1)}$$

$$\alpha = 1.483 + 4.392 r_0 f_c \qquad \text{(C2)}$$

$$\alpha = 1.120 f_c + 5.854 r_0 \qquad \text{(C3)}$$

The coefficients in the equations above were obtained after minimizing the error function using the least standard deviation method, appendix B.

	2D-rough ($n_{2R}=154$)	2D-smooth ($n_{2S}=64$)	3D-rough ($n_{3R}=50$)	3D-smooth ($n_{3S}=17$)
(13)	0.392	(-)	0.462	(-)
(C1)	0.329	0.430	0.547	0.856
(C2)	0.353	0.270	0.458	0.852
(C3)	0.313	0.328	0.526	0.721

Table C1 Standard deviation of α based on 'measured' values of r_0

It is noted that the 'measured' α is based on measured parameters (Q, h_0, B, Δ, t_1, d_{50}) and determined with equation (1). The kinematic viscosity is supposed to be equal to $\nu = 10^{-6} m^2/s$, whereas the depth-averaged critical flow-velocity according to Shields is computed as discussed in section 3 (van Rijn, 1984).
The results of the standard deviation of α are given in table C1.
The optimization shows that the error rate for each relation including equation (13)

	2D-rough ($n_{2R}=154$)	2D-smooth ($n_{2S}=64$)	3D-rough ($n_{3R}=50$)	3D-smooth ($n_{3S}=17$)
(13)	0.448	(-)	1.060	(-)
(C1)	0.307	0.446	0.596	0.568
(C2)	0.395	0.291	0.487	0.735
(C3)	0.326	0.340	0.550	0.574

Table C2 Standard deviation of α based on calculated values of r_0 ($\beta_k=0.5$)

introduced by Jorissen and Vrijling (1989) is of the same order. Generally the error rate for three-dimensional flow is somewhat larger than for two-dimensional flow, especially for hydraulically-smooth conditions.

Table C2 presents the standard deviation of α , which is based on r_0 computed using equation 12. Hence the following remarks can be made.

Considering the model relations C1 to C3 the difference between the calculated and measured standard deviation of r_0 are marginal. However, for 3D-smooth cases

	β_k	2D-rough ($n_{2R}=240$)	2D-smooth ($n_{2S}=132$)	3D-rough ($n_{3R}=54$)	3D-smooth ($n_{3S}=104$)
(13)	0.357	0.411	(-)	1.090	(-)
	0.500	0.441	(-)	1.060	(-)
	0.596	0.468	(-)	1.042	(-)
(C1)	0.357	0.329	0.563	0.682	0.598
	0.500	0.301	0.572	0.596	0.520
	0.596	0.299	0.578	0.555	0.492
(C2)	0.357	0.374	0.268	0.566	0.645
	0.500	0.387	0.271	0.487	0.554
	0.596	0.404	0.275	0.447	0.509
(C3)	0.357	0.306	0.470	0.635	0.633
	0.500	0.313	0.473	0.550	0.541
	0.596	0.335	0.475	0.511	0.498

Table C3 Standard deviation of α based on calculated values of r_0

(three-dimensional flow and hydraulically-smooth conditions) the error rate becomes smaller when the turbulence intensity is calculated, which is probably due to the measuring procedure, as discussed in section 4.4.
Finally the influence of the coefficient β_k (equation 12) on the standard deviation α is determined using approximately 525 experiments (Delft Hydraulics, 1972; Dietz, 1969; Buchko, 1986 and Hoffmans, 1990), table C3. From this analysis it can be concluded that equation C2 (or equation 14) gives the best results compared to the other relations including equation (13).

Appendix D **Verification of the relative turbulence intensity**

report	series	condition	D/h_0	L/h_0	C	$r_{0,m}$	$r_{0,c}$
m648b	s8-20	smooth2D	.00	10.	70.	.06	.05
m648b	s8-21	smooth2D	.00	10.	71.	.08	.05
m648b	s8-22	smooth2D	.00	10.	72.	.06	.05
m648b	s8-25	smooth2D	.00	10.	70.	.08	.05
m648b	s8-24	smooth2D	.00	10.	71.	.08	.05
m648b	s8-64	smooth2D	.00	10.	62.	.06	.06
m648b	s8-63	smooth2D	.00	10.	63.	.07	.06
m648b	s8-61	smooth2D	.00	10.	65.	.06	.06
m648b	s8-62	smooth2D	.00	10.	66.	.07	.06
m648b	s8-60	smooth2D	.00	10.	67.	.08	.06
m648b	s8-59	smooth2D	.00	10.	68.	.07	.06
m648b	s8-58	smooth2D	.00	10.	69.	.08	.05
m648b	s8-56	smooth2D	.00	10.	71.	.08	.05
m648b	s8-31D	smooth2D	.00	10.	65.	.06	.06
m648b	s8-31A	smooth2D	.00	10.	66.	.04	.06
m648b	s8-33B	smooth2D	.00	10.	67.	.06	.06
m648b	s8-49	smooth2D	.00	10.	70.	.07	.05
m648b	s8-53	smooth2D	.00	10.	71.	.06	.05
m648b	s8-52	smooth2D	.00	10.	72.	.06	.05
m648b	s8-54	smooth2D	.00	10.	73.	.07	.05
m648b	s11-3	rough2D	.33	4.	41.	.20	.22
m648b	s11-1	rough2D	.33	4.	41.	.22	.22
m648b	s11-2A	rough2D	.33	4.	41.	.22	.22
m648b	s11-27	rough2D	.33	4.	40.	.23	.22
m648b	s11-29	rough2D	.33	4.	40.	.23	.22
m648b	s11-28	rough2D	.33	4.	40.	.24	.22
m648b	s11-18	rough2D	.33	4.	41.	.20	.22

report	series	condition	D/h_0	L/h_0	C	r_{0m}	r_{0c}
m648b	s11-15	rough2D	.33	4.	41.	.22	.22
m648b	s13-11	rough2D	.50	4.	38.	.32	.30
m648b	s13-10	rough2D	.50	4.	38.	.30	.30
m648b	s13-9	rough2D	.50	4.	38.	.28	.30
m648b	s13-8A	rough2D	.50	4.	38.	.31	.30
m648b	s13-7	rough2D	.50	4.	38.	.31	.30
m648b	s13-6	rough2D	.50	4.	38.	.28	.30
m648b	s13-3	rough2D	.50	4.	38.	.31	.30
m648b	s13-2	rough2D	.50	4.	38.	.29	.30
m648b	s13-1	rough2D	.50	4.	38.	.30	.30
m648b	s14-4	rough2D	.00	10.	36.	.10	.10
m648b	s14-1	rough2D	.00	10.	36.	.09	.10
m648b	s14-2	rough2D	.00	10.	36.	.09	.10
m648b	s14-3	rough2D	.00	10.	36.	.09	.10
m648b	s14-8	rough2D	.00	10.	36.	.12	.10
m648b	s14-7	rough2D	.00	10.	36.	.12	.10
m648b	s14-5A	rough2D	.00	10.	36.	.12	.10
m648b	s15-13	rough2D	.00	10.	39.	.09	.10
m648b	s15-14	rough2D	.00	10.	39.	.10	.10
m648b	s15-15	rough2D	.00	10.	39.	.09	.10
m648b	s15-11	rough2D	.00	10.	39.	.09	.10
m648b	s15-12	rough2D	.00	10.	39.	.09	.10
m648b	s15-9	rough2D	.00	10.	39.	.10	.10
m648b	s15-8	rough2D	.00	10.	39.	.09	.10
m648b	s15-5	rough2D	.00	10.	39.	.09	.10
m648b	s15-7	rough2D	.00	10.	39.	.09	.10
m648b	s15-6	rough2D	.00	10.	39.	.10	.10

report	series	condition	D/h_0	L/h_0	C	$r_{0.m}$	$r_{0.c}$
m648b	s15-4	rough2D	.00	10.	39.	.08	.10
m648b	s15-1	rough2D	.00	10.	39.	.08	.10
m648b	s15-2	rough2D	.00	10.	39.	.09	.10
m648b	s15-3	rough2D	.00	10.	39.	.08	.10
m648b	s15-29	rough2D	.00	10.	39.	.09	.10
m648b	s15-30	rough2D	.00	10.	39.	.08	.10
m648b	s15-31	rough2D	.00	10.	39.	.09	.10
m648b	s15-27	rough2D	.00	10.	39.	.10	.10
m648b	s15-26	rough2D	.00	10.	39.	.11	.10
m648b	s15-25	rough2D	.00	10.	39.	.10	.10
m648b	s15-23A	rough2D	.00	10.	39.	.09	.10
m648b	s15-36	rough2D	.00	10.	39.	.09	.10
m648b	s15-32	rough2D	.00	10.	39.	.10	.10
m648b	s15-33	rough2D	.00	10.	39.	.09	.10
m648b	s15-34	rough2D	.00	10.	39.	.09	.10
m648b	s16A-13	rough2D	.17	4.	41.	.15	.18
m648b	s16A-14	rough2D	.17	4.	41.	.15	.17
m648b	s16A-15	rough2D	.17	4.	41.	.15	.17
m648b	s16A-35	rough2D	.17	4.	41.	.13	.17
m648b	s16A-31	rough2D	.17	4.	41.	.13	.17
m648b	s16A-30A	rough2D	.17	4.	41.	.13	.17
m648b	s16A-33	rough2D	.17	4.	41.	.14	.17
m648b	s16A-32	rough2D	.17	4.	41.	.13	.17
m648b	s16A-23	rough2D	.17	4.	41.	.13	.17
m648b	s16A-24	rough2D	.17	4.	41.	.14	.17
m648b	s16A-20	rough2D	.17	4.	41.	.13	.18
m648b	s16A-19	rough2D	.17	4.	41.	.13	.18

report	series	condition	D/h_0	L/h_0	C	r_{0m}	r_{0c}
m648b	s16A-21	rough2D	.17	4.	41.	.13	.18
m648b	s16A-18	rough2D	.17	4.	41.	.12	.18
m648b	s16A-17	rough2D	.17	4.	41.	.13	.17
m648b	s16A-25	rough2D	.17	4.	40.	.11	.18
m648b	s16A-26	rough2D	.17	4.	40.	.11	.18
m648b	s16A-27	rough2D	.17	4.	41.	.11	.18
m648b	s16B-10	rough2D	.17	4.	41.	.12	.18
m648b	s16B-11	rough2D	.17	4.	41.	.13	.17
m648b	s16B-12	rough2D	.17	4.	41.	.13	.17
m648b	s16B-9	rough2D	.17	4.	41.	.12	.18
m648b	s16B-7	rough2D	.17	4.	41.	.13	.17
m648b	s16B-6	rough2D	.17	4.	41.	.12	.18
m648b	s16B-5	rough2D	.17	4.	41.	.13	.17
m648b	s16B-4	rough2D	.17	4.	41.	.13	.17
m648b	s16B-3	rough2D	.17	4.	41.	.13	.18
m648b	s16B-2	rough2D	.17	4.	41.	.12	.17
m648b	s16B-1	rough2D	.17	4.	41.	.13	.17
m648b	s17A-23A	rough2D	.33	4.	41.	.24	.22
m648b	s17A-13	rough2D	.33	4.	41.	.21	.22
m648b	s17A-12	rough2D	.33	4.	41.	.23	.22
m648b	s17A-11	rough2D	.33	4.	41.	.22	.22
m648b	s17A-9	rough2D	.33	4.	41.	.25	.22
m648b	s17A-20	rough2D	.33	4.	40.	.19	.22
m648b	s17A-16A	rough2D	.33	4.	40.	.20	.22
m648b	s17A-17	rough2D	.33	4.	40.	.20	.22
m648b	s17A-18	rough2D	.33	4.	41.	.20	.22
m648b	s17B-5	rough2D	.33	4.	41.	.24	.22

report	series	condition	D/h_0	L/h_0	C	r_{0m}	r_{0c}
m648b	s17B-6A	rough2D	.33	4.	41.	.21	.22
m648b	s17B-4	rough2D	.33	4.	41.	.19	.22
m648b	s17B-3	rough2D	.33	4.	41.	.16	.22
m648b	s17B-2	rough2D	.33	4.	41.	.20	.22
m648b	s17B-22	rough2D	.33	4.	40.	.22	.22
m648b	s19-11	rough2D	.00	12.	41.	.07	.09
m648b	s19-10	rough2D	.00	12.	41.	.08	.09
m648b	s19-7A	rough2D	.00	12.	41.	.07	.09
m648b	s19-9A	rough2D	.00	12.	41.	.07	.09
m648b	s19-4	rough2D	.00	12.	41.	.10	.09
m648b	s19-5	rough2D	.00	12.	41.	.10	.09
m648b	s19-6	rough2D	.00	12.	41.	.10	.09
m648b	s19-1	rough2D	.00	12.	41.	.10	.09
m648b	s19-2	rough2D	.00	12.	41.	.09	.09
m648b	s19-3	rough2D	.00	12.	41.	.11	.09
m648b	s19-20	rough2D	.00	12.	43.	.07	.09
m648b	s19-17	rough2D	.00	12.	43.	.06	.09
m648b	s19-21	rough2D	.00	12.	43.	.06	.09
m648b	s19-18	rough2D	.00	12.	43.	.06	.09
m648b	s19-22A	rough2D	.00	12.	41.	.07	.09
m648b	s19-23	rough2D	.00	12.	41.	.07	.09
m648b	s19-24	rough2D	.00	12.	41.	.08	.09
m648b	s19-25A	rough2D	.00	12.	41.	.08	.09
m648b	s19-D	rough2D	.00	12.	41.	.08	.09
m648b	s19-C	rough2D	.00	12.	41.	.08	.09
m648b	s19-B	rough2D	.00	12.	41.	.09	.09
m648b	s19-A	rough2D	.00	12.	41.	.09	.09

report	series	condition	D/h_0	L/h_0	C	r_{0m}	r_{0c}
m648b	s20-9	rough2D	.23	5.	41.	.13	.18
m648b	s20-10	rough2D	.23	5.	41.	.16	.18
m648b	s20-5	rough2D	.23	5.	41.	.15	.18
m648b	s20-4	rough2D	.23	5.	41.	.16	.18
m648b	s20-6	rough2D	.23	5.	41.	.17	.18
m648b	s21-3	rough2D	.33	5.	41.	.23	.21
m648b	s21-2	rough2D	.33	5.	41.	.21	.21
m648b	s22-5	smooth2D	.00	12.	74.	.04	.05
m648b	s22-6	smooth2D	.00	12.	75.	.04	.05
m648b	s22-3	smooth2D	.00	12.	80.	.06	.05
m648b	s22-4	smooth2D	.00	12.	82.	.06	.05
m648b	s22-1	smooth2D	.00	12.	88.	.05	.04
m648b	s22-8	smooth2D	.00	12.	65.	.04	.06
m648b	s22-9	smooth2D	.00	12.	65.	.03	.06
m648b	s22-10	smooth2D	.00	12.	66.	.04	.06
m648b	s23-6	smooth2D	.00	2.	63.	.03	.06
m648b	s23-5	smooth2D	.00	2.	64.	.03	.06
m648b	s23-4	smooth2D	.00	2.	65.	.02	.06
m648b	s23-3	smooth2D	.00	2.	65.	.02	.06
m648b	s24-4	smooth2D	.00	8.	63.	.04	.06
m648b	s24-3	smooth2D	.00	8.	64.	.03	.06
m648b	s24-2	smooth2D	.00	8.	65.	.05	.06
m648b	s24-1	smooth2D	.00	8.	65.	.05	.06
m648b	s25-4	smooth2D	.00	14.	63.	.04	.06
m648b	s25-3	smooth2D	.00	14.	64.	.05	.06
m648b	s25-2	smooth2D	.00	14.	65.	.06	.06
m648b	s25-1	smooth2D	.00	14.	65.	.05	.06

report	series	condition	D/h_0	L/h_0	C	r_{0m}	r_{0c}
m648b	s25-5	smooth2D	.00	14.	66.	.04	.06
m648b	s26-3	smooth2D	.00	14.	56.	.04	.07
m648b	s26-2	smooth2D	.00	14.	57.	.04	.07
m648b	s26-1	smooth2D	.00	14.	57.	.05	.07
m648b	s26-4	smooth2D	.00	14.	57.	.04	.07
m648b	s27-4	smooth2D	.00	14.	53.	.04	.07
m648b	s27-3	smooth2D	.00	14.	53.	.05	.07
m648b	s27-2	smooth2D	.00	14.	53.	.05	.07
m648b	s27-1	smooth2D	.00	14.	53.	.05	.07
m648b	s28-4	smooth2D	.00	14.	49.	.05	.08
m648b	s28-3	smooth2D	.00	14.	49.	.04	.08
m648b	s28-2	smooth2D	.00	14.	49.	.05	.08
m648b	s28-1	smooth2D	.00	14.	49.	.05	.08
m648b	s29-5	smooth2D	.00	14.	44.	.06	.09
m648b	s29-4	smooth2D	.00	14.	44.	.05	.09
m648b	s29-3	smooth2D	.00	14.	44.	.05	.09
m648b	s29-2	smooth2D	.00	14.	44.	.06	.09
m648b	s29-1	smooth2D	.00	14.	44.	.05	.09
m648b	s30-5	rough2D	.00	14.	39.	.06	.10
m648b	s30-4	rough2D	.00	14.	39.	.06	.10
m648b	s30-3	rough2D	.00	14.	39.	.06	.10
m648b	s30-2	rough2D	.00	14.	39.	.06	.10
m648b	s30-1	rough2D	.00	14.	39.	.06	.10
m648b	s31-5	rough2D	.00	14.	34.	.07	.11
m648b	s31-3	rough2D	.00	14.	34.	.07	.11
m648b	s31-1	rough2D	.00	14.	34.	.08	.11
m847b	S0GLAD	smooth2D	.00	10.	73.	.04	.05

report	series	condition	D/h_0	L/h_0	C	$r_{0,m}$	$r_{0,c}$
m847b	S0M0L0	rough2D	.00	10.	46.	.07	.08
m847b	S0M1L2	smooth2D	.00	10.	75.	.07	.05
m847b	S0M0L0	rough2D	.00	10.	46.	.08	.08
m847b	S0M1L2	smooth2D	.00	10.	73.	.07	.05
m847b	S1GLAD	smooth2D	.30	10.	71.	.10	.15
m847b	S1M0L0	rough2D	.30	10.	46.	.13	.16
m847b	S1M1L2	smooth2D	.30	10.	73.	.14	.15
m847b	S1M0L0	rough2D	.30	10.	46.	.14	.16
m847b	S2GLAD	smooth2D	.60	10.	70.	.20	.27
m847b	S2M0L0	rough2D	.60	10.	46.	.22	.27
m847c	F0V1M	rough3D	.00	5.	46.	.08	.08
m847c	F0V1M	rough3D	.00	5.	46.	.08	.08
m847c	F0V1M	rough3D	.00	5.	47.	.08	.08
m847c	F0V1M	rough3D	.00	5.	47.	.08	.08
m847c	F1V1M	rough3D	.30	5.	46.	.12	.19
m847c	F1V1M	rough3D	.30	5.	46.	.12	.19
m847c	F1V1M	rough3D	.30	5.	46.	.12	.19
m847c	F2V1M	rough3D	.60	5.	45.	.48	.35
m847c	F2V1M	rough3D	.60	5.	45.	.48	.35
m847c	F2V1M	rough3D	.60	5.	46.	.48	.35
m847c	F0V2M	rough3D	.00	10.	46.	.14	.08
m847c	F0V2M	rough3D	.00	10.	46.	.14	.08
m847c	F0V2M	rough3D	.00	10.	47.	.14	.08
m847c	F0V2M	rough3D	.00	10.	47.	.14	.08
m847c	F1V2M	rough3D	.30	10.	46.	.14	.16
m847c	F1V2M	rough3D	.30	10.	46.	.14	.16
m847c	F1V2M	rough3D	.30	10.	46.	.14	.16

report	series	condition	D/h_0	L/h_0	C	$r_{0,m}$	$r_{0,c}$
m847c	F1V2M	rough3D	.30	10.	46.	.14	.16
m847c	F2V2M	rough3D	.60	10.	46.	.32	.27
m847c	F2V2M	rough3D	.60	10.	46.	.32	.27
m847c	F2V2M	rough3D	.60	10.	46.	.32	.27
m847c	F0V3M	rough3D	.00	15.	47.	.12	.08
m847c	F0V3M	rough3D	.00	15.	47.	.12	.08
m847c	F0V4M	rough3D	.00	20.	47.	.13	.08
m847c	F0V4M	rough3D	.00	20.	47.	.13	.08
m847c	F0V4M	rough3D	.00	20.	47.	.13	.08
m847c	F1V4M	rough3D	.30	20.	46.	.17	.13
m847c	F1V4M	rough3D	.30	20.	47.	.17	.13
m847c	F1V4M	rough3D	.30	20.	47.	.17	.13
m847c	F2V4M	rough3D	.60	20.	46.	.17	.21
m847c	F2V4M	rough3D	.60	20.	46.	.17	.21
m847c	F2V4M	rough3D	.60	20.	46.	.17	.21
m847c	D0V1G	smooth3D	.00	5.	65.	.08	.06
m847c	D0V1G	smooth3D	.00	5.	66.	.08	.06
m847c	D1V1G	smooth3D	.30	5.	65.	.18	.18
m847c	D1V1G	smooth3D	.30	5.	66.	.18	.18
m847c	D2V1G	smooth3D	.60	5.	65.	.19	.34
m847c	D0V2G	smooth3D	.00	10.	65.	.10	.06
m847c	D0V2G	smooth3D	.00	10.	66.	.10	.06
m847c	D0V2G	smooth3D	.00	10.	67.	.10	.06
m847c	D1V2G	smooth3D	.30	10.	63.	.12	.15
m847c	D1V2G	smooth3D	.30	10.	65.	.12	.15
m847c	D1V2G	smooth3D	.30	10.	66.	.12	.15
m847c	D2V2G	smooth3D	.60	10.	61.	.36	.27

report	series	condition	D/h_0	L/h_0	C	$r_{0,m}$	$r_{0,c}$
m847c	D2V2G	smooth3D	.60	10.	63.	.36	.27
m847c	D2V2G	smooth3D	.60	10.	65.	.36	.27
m847c	D0V4G	smooth3D	.00	20.	74.	.15	.05
m847c	D1V4G	smooth3D	.30	20.	74.	.12	.12
m847c	D2V4G	smooth3D	.60	20.	74.	.20	.20
m847c	D0V1R	rough3D	.00	5.	42.	.12	.09
m847c	D0V1R	rough3D	.00	5.	42.	.12	.09
m847c	D0V1R	rough3D	.00	5.	42.	.12	.09
m847c	D1V1R	rough3D	.30	5.	42.	.18	.20
m847c	D1V1R	rough3D	.30	5.	42.	.18	.20
m847c	D2V1R	rough3D	.60	5.	42.	.46	.35
m847c	D0V2R	rough3D	.00	10.	42.	.16	.09
m847c	D0V2R	rough3D	.00	10.	42.	.16	.09
m847c	D0V2R	rough3D	.00	10.	42.	.16	.09
m847c	D1V2R	rough3D	.30	10.	42.	.18	.17
m847c	D1V2R	rough3D	.30	10.	42.	.18	.17
m847c	D1V2R	rough3D	.30	10.	42.	.18	.17
m847c	D2V2R	rough3D	.60	10.	42.	.40	.28
m847c	D2V2R	rough3D	.60	10.	42.	.40	.28
m847c	D2V2R	rough3D	.60	10.	42.	.40	.28
m847c	D0V4R	rough3D	.00	20.	42.	.18	.09
m847c	D1V4R	rough3D	.30	20.	42.	.18	.14
m847c	D2V4R	rough3D	.60	20.	42.	.28	.21
q239	t01	rough2D	.00	8.	43.	.05	.09
q239	t02	rough2D	.00	8.	43.	.05	.09
q239	t03	rough2D	.00	8.	43.	.05	.09
q239	t04	rough2D	.00	8.	40.	.06	.09

report	series	condition	D/h_0	L/h_0	C	r_{0m}	r_{0c}
q239	t05	rough2D	.00	8.	40.	.06	.09
q239	t06	rough2D	.00	8.	40.	.06	.09
q239	t07	rough2D	.34	4.	40.	.21	.22
q239	t08	rough2D	.34	4.	40.	.21	.22
q239	t09	rough2D	.34	2.	40.	.21	.25
q239	t10	rough2D	.34	1.	40.	.21	.27
q239	t11	rough2D	.34	4.	40.	.21	.22
q239	t12	rough2D	.35	4.	43.	.16	.22
q239	t13	rough2D	.35	4.	43.	.16	.22
q239	t14	rough2D	.35	4.	43.	.16	.22
q239	t15	rough2D	.35	4.	43.	.16	.22
q239	t16	rough2D	.35	4.	43.	.16	.22
q239	t17	rough2D	.35	4.	43.	.16	.22
q239	t18	rough2D	.35	4.	43.	.16	.22
q239	t19	rough2D	.00	9.	40.	.05	.09

References

Breusers, H.N.C., 1966, Conformity and time scale in two-dimensional local scour, Proceedings Symposium on model and prototype conformity, Hydraulic Research Laboratory, Poona, p.1-8.

Breusers, H.N.C., 1967, Time scale of two-dimensional local scour, 12th IAHR congress, Vol.3, Paper C32, Fort Collins, Colorado.

Breusers, H.N.C. and A.J. Raudkivi, 1991, Scouring, Hydraulic structures design manual, IAHR, A.A. Balkema, Rotterdam.

Buchko, M.F., 1986, Investigation of local scour in cohesionless sediments by using a tunnel model, Report No.Q239, Delft Hydraulics.

Delft Hydraulics, 1972, Systematical investigation of two and three-dimensional local scour, Investigation M648/M863/M847/M1533 (in dutch), Delft Hydraulics, Delft.

Dietz, J.W. 1969, Kolkbildung in feinen oder leichten Sohlmaterialien bei strömendem Abfluß, Mitteilungen Heft 155, Universität Fridericiana Karlsruhe.

Driegen, J., T. van der Meulen and J.L.M. Konter, 1987, Evaluation of scour experiments at prototype scale (in dutch), Report No.Q496, Delft Hydraulics, Delft.

Graauw, A.F.F. de, and K.W. Pilarczyk, 1981, Model-prototype conformity of local scour in non-cohesive sediments beneath overflow-dam, 19th IAHR-congress, New Delhi.

Jorissen, R.E. and J.K. Vrijling, 1989, Local scour downstream of hydraulic constructions, Proceedings 23rd IAHR-Congress, Ottawa, p.B433-B440.

Hinze, J.O., 1961, Sediment transport caused by turbulence, unpublished notes (in dutch), Delft Hydraulics, Delft.

Hinze, J.O., 1975, Turbulence, Second edition, McGraw-Hill Book company, New York.

Hoffmans, G.J.C.M., 1990, Concentration and flow velocity measurements in a local scour hole, Report No.4-90, Faculty of Civil Engineering, Hydraulic and Geotechnical Engineering Division, Delft University of Technology, Delft.

Hoffmans, G.J.C.M., 1992, Two-dimensional mathematical modelling of local-scour holes, Doctoral thesis, Faculty of Civil Engineering, Hydraulic and Geotechnical Engineering Division, Delft University of Technology, Delft.

Launder, B.E. and D.B. Spalding, 1972, Mathematical models of turbulence, Academic Press, London.

Meulen, T. van der, and J.J. Vinjé, 1975, Three-dimensional local scour in non-cohesive sediments, 16th IAHR-Congress, Sao Paulo.

Mierlo, M.C.L.M. van, and J.C.C. de Ruiter, 1988, Turbulence measurements above dunes, Report No.Q789, Vol.1 and 2, Delft Hydraulics, Delft.

Neill, C.R., 1968, A re-examination of the beginning of movement for coarse granular bed materials, Hydraulic Research Station, Wallingford.

Nezu, I., 1977, Turbulent structure in open-channel flows (translation of Doctoral dissertation published in japanese), Department of Civil Engineering, Kyoto University, Kyoto.

Prins, J.E., 1963, Échelle du temps dans la réproduction d'un affouillement, La Houille Blanche, No.2, p.183-188.
Rijn, L.C. van, 1982, Equivalent roughness of alluvial bed, Journal of Hydraulic Division, ASCE, Vol.108, p.1215-1218.
Rijn, L.C. van, 1984, Sediment transport, part 1: Bed load transport, Journal of Hydraulic Engineering, ASCE, Vol.110, No.10, p.1431-1456.
Rodi, W., 1980, Turbulence models and their application in hydraulics, IAHR-section on Fundamentals of Division 2, Delft.
Thijsse, J.Th., 1949, Formulae for the friction head loss along conduit walls under turbulent flow, 3rd meeting IAHR, Grenoble, paper III-4.
Townsend, A.A., 1976, The structure of turbulent shear flow, Cambridge University Press, Cambridge.
Troutt, T.R., Scheelke, B. and T.R. Norman, 1984, Organized structures in a reattaching separated flow field, Journal of Fluid Mechanics, Vol.143, p.413-427.
Schuyf, J.P., The measurements of turbulent velocity fluctuations with a propellor-type current-meter, Journal of Hydraulic Research, Vol.4.
Vinjé, J.J., 1967, On the flow-characteristics of vortices in three-dimensional local scour, 12th IAHR-congress, Fort Collins, Colorado.
Zanke, U., 1978, Zusammenhänge zwischen Strömung und Sedimenttransport Teil 2: Berechnung des Sedimenttransportes hinter befestigtigten Sohlenstrecken, Sonderfall zweidimensionaler Kolk, Mitteilungen des Franzius-Instituts der TU Hannover, Heft 48.